Available online at www.sciencedirect.com
ScienceDirect
Bioorganic & Medicinal Chemistry 16 (2008) 5103–5108
Bioorganic & Medicinal Chemistry

A CoMSIA study on the adenosine kinase inhibition of pyrrolo[2,3-*d*]pyrimidine nucleoside analogues

Julio Caballero,[a,*] Michael Fernández[b,c] and Fernando D. González-Nilo[a]

[a]*Centro de Bioinformática y Simulación Molecular, Universidad de Talca, 2 Norte 685, Casilla 721, Talca, Chile*
[b]*Molecular Modeling Group, Center for Biotechnological Studies, University of Matanzas, Matanzas, Cuba*
[c]*Department of Bioscience and Bioinformatics, Kyushu Institute of Technology (KIT) 680-4 Kawazu, Iizuka, Fukuoka 820-8502, Japan*

Received 8 January 2008; revised 29 February 2008; accepted 10 March 2008
Available online 14 March 2008

Abstract—The structural requirements of pyrrolo[2,3-*d*]pyrimidine nucleoside (PPN) analogues as adenosine kinase (AK) inhibitors were in silico studied by using CoMSIA method. All models were trained with 32 compounds, after which they were evaluated for predictive ability with additional 5 compounds. Quantitative information on structure–activity trends is provided for further rational development and direction of selective synthesis. The best CoMSIA model included hydrophobic, H-bond donor and H-bond acceptor fields and had a good predictive quality according to internal validation criteria. In addition, this model predicted adequately the compounds contained in the test set. The analysis of the model gives a comprehensive qualitative and quantitative description of the molecular features at C4 and C5 positions of the pyrrolo[2,3-*d*]pyrimidine scaffold and C5-position of the β-D-ribofuranose of PPN analogues, relevant for a high AK inhibitory activity.

1. Introduction

Compounds that activate adenosine receptors, such as adenosine and adenosine receptor agonists, represent potential therapeutic agents for a variety of diseases including epilepsy, diabetes, hypertension, pain, and inflammation.[1] Adenosine receptor agonists are effective in various animal seizure models[2]; however, the side effect profile of these agonists, including significant reductions in blood pressure and heart rate, pronounced hypothermia, and motor depression, is a cause for concern.[3–5] The use of adenosine-regulating agents (ARAs) is an alternative strategy that would harness the potential therapeutic benefits of adenosine receptor activation while minimizing the side effects by enhancing the natural adenosinergic feedback mechanism associated with seizures.[6] ARAs affect the production or metabolism of adenosine such that extracellular adenosine is elevated in a relatively site- and event-specific manner.

Adenosine kinase (AK) has been identified as one potential ARA target.[7] AK is a key enzyme in the regulation of the extracellular adenosine, since it is partly responsible for adenosine's extremely short plasma half-life.[8] According to this, inhibition of AK provokes the increase of intracellular adenosine, which passes out of the cell via passive diffusion or via nucleoside transporters to activate nearby cell-surface adenosine receptors.[9] AK inhibitors (AKIs) have been recognized as potent antiepileptic agents with an improved side effect profile compared with adenosine receptor agonists.[7]

Computational-based rational design of drugs has increased in the last decade. Most of those approaches are focused on quantitative structure–activity relationship (QSAR) studies.[10] A QSAR model is a classical method for establishing some knowledge about ligand requirements for having a potent activity without using receptor's structure. QSAR proposes a mathematically quantified and computerized form from the chemical structure. In this sense, the QSAR conserves resources and accelerates the process of development of new molecules for use as drugs.[11]

As part of an effort to find highly potent AKIs, Ugarkar et al.[12] reported a structure–activity relationship study on pyrrolo[2,3-*d*]pyrimidine nucleoside (PPN) analogues

Keywords: Adenosine kinase inhibitors; In silico drug design; Quantitative structure–activity relationships; CoMSIA.
* Corresponding author. Tel.: +56 71 201 662; fax: +56 71 201 561; e-mail addresses: jcaballero@utalca.cl; jmcr77@yahoo.com

0968-0896/$ - see front matter © 2008 Elsevier Ltd. All rights reserved.
doi:10.1016/j.bmc.2008.03.027

as AKIs. Some QSAR studies have been carried out on these compounds. Srikanth et al.[13] applied the linear free energy relation model of Hansch[14] on this dataset. Authors concluded that electronic distribution on both pyrimidine and pyrrole rings plays a major role in the AK inhibitory activity. In addition, authors found that hydrophobic interactions of the pyrimidine ring have positive effects, and steric bulk on both the rings is not detrimental to the activity. More recently, González and Moldes[15] carried out a QSAR study by using topological sub-structural molecular design (TOPS-MODE) approach[16] and descriptors from Dragon software.[17] Despite the above studies reporting statistically robust QSAR models, the use of simple molecular properties or non-easy interpretable descriptors limits their interpretation as a guide to the synthetic chemists for the designing of new active compounds.

To gain insights into the structural and molecular requirements influencing the AK inhibitory activity of PPN analogues, we describe herein a 3D-QSAR analysis of a dataset of Ugarkar et al.[12] (the chemical structures are shown in Table 1). We used classical comparative molecular similarity index analysis (CoMSIA), which

Table 1. Experimental and predicted inhibitory activities ($\log(10^3/IC_{50})$) of pyrrolo[2,3-*d*]pyrimidine nucleoside (PPN) analogues using model CoMSIA-HDA

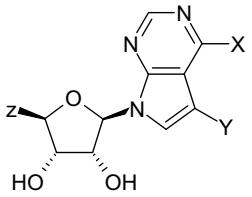

Compound	X	Y	Z	$\log(10^3/IC_{50})$		
				Exp.	Predicted	LOO-predicted
Training set						
1	NH_2	I	CH_2OH	4.59	4.52	4.44
2	NH_2	I	CH_3	5.05	4.85	4.73
3	NH_2	Br	CH_3	4.40	4.53	4.70
4	NH_2	Cl	CH_2OH	3.68	3.82	4.06
5	Cl	I	CH_3	5.52	5.30	5.01
6	Cl	Br	CH_3	4.30	4.50	4.60
7	Cl	CH_3	CH_3	3.27	3.18	2.53
8	Cl	SCH_3	CH_3	4.15	4.09	3.79
9	Cl	I	CH_2N_3	5.05	5.08	5.28
10	Cl	Br	CH_2N_3	4.00	4.11	4.40
11	NH_2	CH_3	CH_3	1.78	1.93	2.22
12	NH_2	SCH_3	CH_3	2.87	2.97	2.95
13	NH_2	CO_2Et	CH_3	3.00	2.99	1.28
14	NH_2	I	CH_2N_3	4.46	4.40	4.08
15	NH_2	Br	CH_2N_3	4.20	4.16	3.45
16	NH_2	I	$CHCH_2$	4.00	3.92	2.56
17	NH_2	I	Et	4.22	4.28	4.23
18	NH_2	Br	Et	3.30	3.20	3.06
19	$NHCH_3$	I	CH_2OH	2.92	2.87	3.54
20	SH	I	CH_3	2.19	—	—
21	SCH_3	I	CH_3	4.35	4.38	4.45
22	*S*-Allyl	I	CH_3	2.55	2.68	3.49
23	*S*-*n*-C_4H_9	I	CH_3	3.00	3.00	2.98
24	*S*-Benzyl	I	CH_3	3.00	2.92	1.84
25	*S*-*p*-NO_2Benzyl	I	CH_3	2.70	2.69	3.85
26	NH_2	I	CH_2NH_2	6.22	6.75	7.52
27	NH_2	Br	CH_2NH_2	6.70	6.23	5.48
28	NH_2	H	CH_2NH_2	1.89	1.82	4.22
29	NH_2	CN	CH_2OH	3.51	3.44	3.27
30	NH_2	CN	CH_3	3.51	3.56	3.88
31	NH_2	$CONH_2$	CH_2OH	3.33	3.37	3.49
32	NH_2	$CONH_2$	CH_3	3.34	3.30	3.17
Test set						
33	NH_2	Br	CH_2OH	3.92	4.18	
34	Cl	I	CH_2OH	4.62	5.64	
35	Cl	I	CH_2OCH_3	3.35	3.98	
36	NH_2	I	CH_2OCH_3	2.92	1.61	
37	Cl	I	CH_2NH_2	7.00	7.16	

may throw some light on the requirements of the substituents for the further development of more potent PPN analogues. Predicitivity of the resultant model was quantified with the cross-validated leave-one-out (LOO) coefficient of determination (Q^2) and the prediction of new compounds (5 compounds).

2. Results and discussion

Figure 1 shows the aligned molecules within the grid box (grid spacing 2.0 Å) used to generate the CoMSIA columns. The alignment ensures a straightforward determination of the relevant effects of substituents at C4 and C5 positions of the pyrrolo[2,3-*d*]pyrimidine and C5-position of β-D-ribofuranose structures.

2.1. CoMSIA results

Firstly, we developed the CoMSIA models by including one field, and then, we combined these fields and analyzed the statistical quality of hybrid models by considering Q^2 values.[18,19] According to this analysis, we detect that compound **20** presented large residuals in all models; in this sense, it was excluded as an outlier. Outliers are those compounds which have unexpected biological activity and are unable to fit in a QSAR model.[20] Outliers can be identified as compounds with significant standard residuals. There are several reasons for their occurrence in QSAR studies; for example, chemicals might be acting by a mechanism different from that of the majority of the dataset. It is also likely that outliers might be a result of a random experimental error that could be significant when analyzing the large datasets.[21] In our context, compound **20** is the only one inhibitor that contains a SH group at C4-position of pyrrolo[2,3-*d*]pyrimidine; in this sense, it can interact with the enzyme by other mechanisms.

The stepwise development of CoMSIA models using different fields, without considering compound **20**, is presented in Table 2. The predictability of the models is the most important criterion for assessment of QSAR methods. CoMSIA models using one field were statistically unacceptable ($Q^2 < 0.5$). At this level, we combined several fields for creating hybrid models. Models encompassing two fields were also statistically unacceptable; however, when hydrophobic and H-bond acceptor fields were included (model CoMSIA-HA), a higher Q^2 value was obtained. We evaluated if the addition of other fields produces an improvement in the internal validation of the model CoMSIA-HA. When the H-bond donor field was added, a CoMSIA model with a better statistical significance was obtained (CoMSIA-HDA). Models including more fields had lower Q^2 values (Table 2).

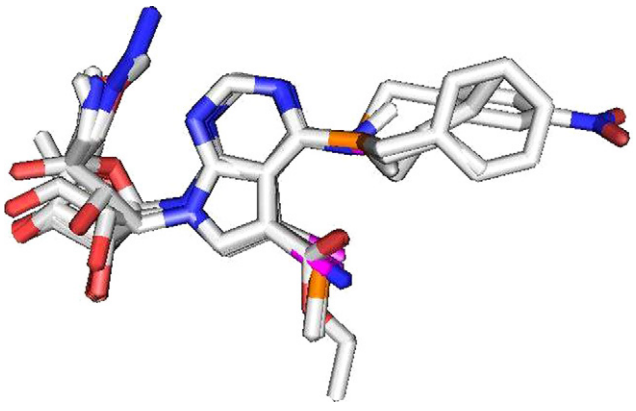

Figure 1. Atom-by-atom superposition used for 3D-QSAR analysis.

The best model (CoMSIA-HDA) reveals that hydrophobic, H-bond donor and H-bond acceptor fields have a major influence in the AK inhibitory activity. This model has a Q^2 value of 0.563 using 17 components, explains 97.9% of the variance, has a low standard deviation ($s = 0.247$), and a high Fisher ratio ($F = 35.88$). The predictions of $\log(10^3/IC_{50})$ values for the 31 PPN analogues using model CoMSIA-HDA are shown in Table 1. The correlation between the calculated and experimental values of $\log(10^3/IC_{50})$ (from training and LOO cross-validation) is shown in Figure 2.

We also used model CoMSIA-HDA to predict the opioid activities of the test set compounds. The values are given in Table 1 and correlation between the calculated and experimental values are represented in Figure 2. This analysis reveals that the proposed model also predicted adequately all the compounds in the test set.

The progressive scrambling procedure was applied to determine the sensitivity of the model to small systematic perturbations of the response variable.[22] In this method, the rows are sorted with respect to the dependent variable and then they are partitioned in a number of specific bins. Within each bin, the dependent variables are scrambled a number of times, and each such scrambling is characterized in terms of the correlation of the scrambled responses with the unperturbed data (R^2_{scr}). The standard error of prediction and the cross-validated correlation coefficient (Q^2_{scr}) as a function of R^2_{scr} at this binning level are obtained. This process is repeated by decreasing the number of bins by 1 upto a defined minimum number of bins. QSAR models which are unstable (which change greatly with small changes in underlying response values) are characterized by slopes dQ^2_{scr}/dR^2_{scr} greater than 1.20. Stable models (which change proportionally with small changes in underlying data) have slopes near 1.00. When we applied the progressive scrambling procedure to the CoMSIA-HDA model, we found a dQ^2_{scr}/dR^2_{scr} value of 1.12.

2.2. Interpretation of the best CoMSIA model

The contour plot of the CoMSIA hydrophobic, H-bond donor and those of the H-bond acceptor fields (stedv * coeff) are presented in Figure 3. Favored and disfavored levels fixed at 80% and 20%, respectively, were used. The active compound **26** is shown inside the fields. Ugarkar et al.[12] found that a halogen atom such as Cl, Br, or I at the C5-position and either a Cl, NH_2 or SCH_3 group at the C4-position of the pyrrolo[2,3-*d*]-pyrimidine ring

Table 2. Results of the CoMSIA analysis using several different field combinations[a]

	NC	R^2	s	F	Q^2	s_{CV}	Fraction				
							Steric	Electrostatic	Hydrophobic	H-bond donor	H-bond acceptor
CoMSIA-S	2	0.287	0.984	5.63	0.102	1.104	1				
CoMSIA-E	14	0.960	0.309	27.29	0.316	1.275		1			
CoMSIA-H	4	0.558	0.803	8.22	0.278	1.028			1		
CoMSIA-D	2	0.229	1.023	4.16	−0.180	1.266				1	
CoMSIA-A	1	0.165	1.046	5.74	0.032	1.126					1
CoMSIA-SE	18	0.965	0.332	18.52	0.199	1.593	0.184	0.816			
CoMSIA-EH	20	0.979	0.283	21.43	0.210	1.733		0.548	0.452		
CoMSIA-HA	5	0.717	0.656	12.64	0.378	1.029			0.625		0.375
CoMSIA-EHA	4	0.728	0.630	17.43	0.204	1.079		0.342	0.505		0.153
CoMSIA-HDA	**17**	**0.979**	**0.247**	**35.88**	**0.563**	**1.318**			**0.381**	**0.452**	**0.167**
CoMSIA-SHDA	19	0.983	0.241	33.87	0.523	1.336	0.097		0.334	0.434	0.136
CoMSIA-EHDA	2	0.471	0.847	12.47	0.162	1.066		0.187	0.439	0.289	0.085
CoMSIA-ALL	20	0.985	0.241	32.27	0.294	1.638	0.076	0.196	0.262	0.367	0.099

[a] All the models consider compound **20** as an outlier. NC is the number of components from PLS analysis, R^2 is the square of correlation coefficient, s is the standard deviation of the regression, F is the Fisher ratio, Q^2 and s_{CV} are the correlation coefficient and standard deviation of the leave-one-out (LOO) cross-validation, respectively. The best models are indicated in boldface.

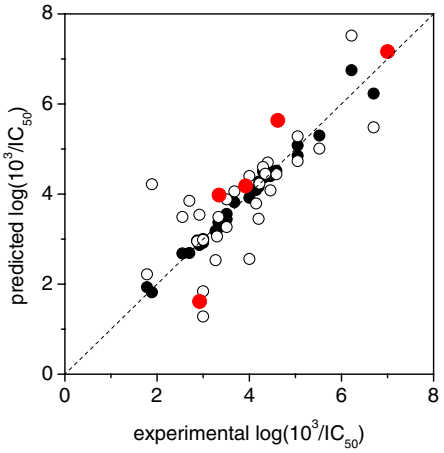

Figure 2. Scatter plot of the experimental activities versus predicted activities for model CoMSIA-HDA: (●) training set predictions (○) LOO cross-validated predictions (●) test set predictions.

system are essential for PPN analogues to potently inhibit AK; while the C5-position of β-D-ribofuranose appears to accommodate both hydrophobic and hydrophilic groups, with the amino group at this position resulting in the most potent AK inhibitors. Although 3D structure of human AK has been determined by X-ray crystallography,[23] the binding orientation of the inhibitors is unknown, and authors could not interpret the structure–activity trends according to the interactions between the inhibitors and the enzyme.[12] The analysis of the isopleths in the contour plots allows interpreting the structure–activity relationship in this dataset without considering the enzyme structure.

The well-tolerated hydrophobic groups are shown as yellow contours (Fig. 3B). A narrow yellow isopleth is found around the substituents at C4 and C5 positions of the pyrrolo[2,3-*d*]pyrimidine scaffold. This isopleth detects that Cl at C4-position and I at C5-position favour the AK inhibitory activity. Otherwise, white contours represent zones where hydrophobic groups are not tolerated. Several white isopleths are located in the outer part of C4 and C5 positions of the pyrrolo[2,3-*d*]pyrimidine and C5-position of β-D-ribofuranose. This can be ascribed to the fact that large hydrophobic groups at these positions deteriorate the AK inhibitory activity. When NH_2 or Cl groups at C4-position of the pyrrolo[2,3-*d*]pyrimidine in compounds **2** and **5** are substituted by large hydrophobic groups (compounds **22**–**25**), the AK inhibitory activity decreases from $\log(10^3/IC_{50})$ above 5 to $\log(10^3/IC_{50}) \sim 3$. When I at C5-position of the pyrrolo[2,3-*d*]pyrimidine in compounds **2** and **5** is substituted by SCH_3 or CO_2Et groups (compounds **12**, **13** and **8**), the AK activity decreases to $\log(10^3/IC_{50}) \sim 3$ or 4. Meanwhile, compounds with CH_2OH, CH_3, CH_2N_3 and CH_2NH_2 at C5-position of the β-D-ribofuranose are more active than compounds with the larger hydrophobic CH_2OCH_3 at this position (compounds **1**, **2**, **5**, **9**, **14**, **26**, **34** and **37** have a $\log(10^3/IC_{50})$ value above 4.4, while compounds **35** and **36** have $\log(10^3/IC_{50}) = 3.35$ and 2.92, respectively).

The graphical interpretation of the field contributions of the H-bonding properties are shown in Figure 3C (H-bond donor field) and 3d (H-bond acceptor field). Two cyan isopleths are located near C4-position of pyrrolo-[2,3-*d*]pyrimidine (Fig. 3C), which represent areas where H-bond donors favor the AK inhibitory activity. PPNs which contain NH_2 group at this position have a high potency as AKIs. In that respect, methylation of this group in compound **1** ($\log(10^3/IC_{50}) = 4.59$) results in the less active compound **19** ($\log(10^3/IC_{50}) = 2.92$). Otherwise, two purple isopleths are found in a more external region from C4-position and near C5-position of the pyrrolo[2,3-*d*]pyrimidine; they identified areas where H-bond donors reduce the AK inhibitory activity. According to these contours, groups containing polar hydrogens are disfavored in a more external region of C4-position, and groups containing H-bond donor atoms such as $CONH_2$ (compounds **31** and **32**) are disfavored at C5-position. With respect to H-bond acceptor CoMSIA field, a sole magenta isopleth is located near C5-position of the pyrrolo[2,3-*d*]pyrimidine (Fig. 3D), which represents areas where H-bond accep-

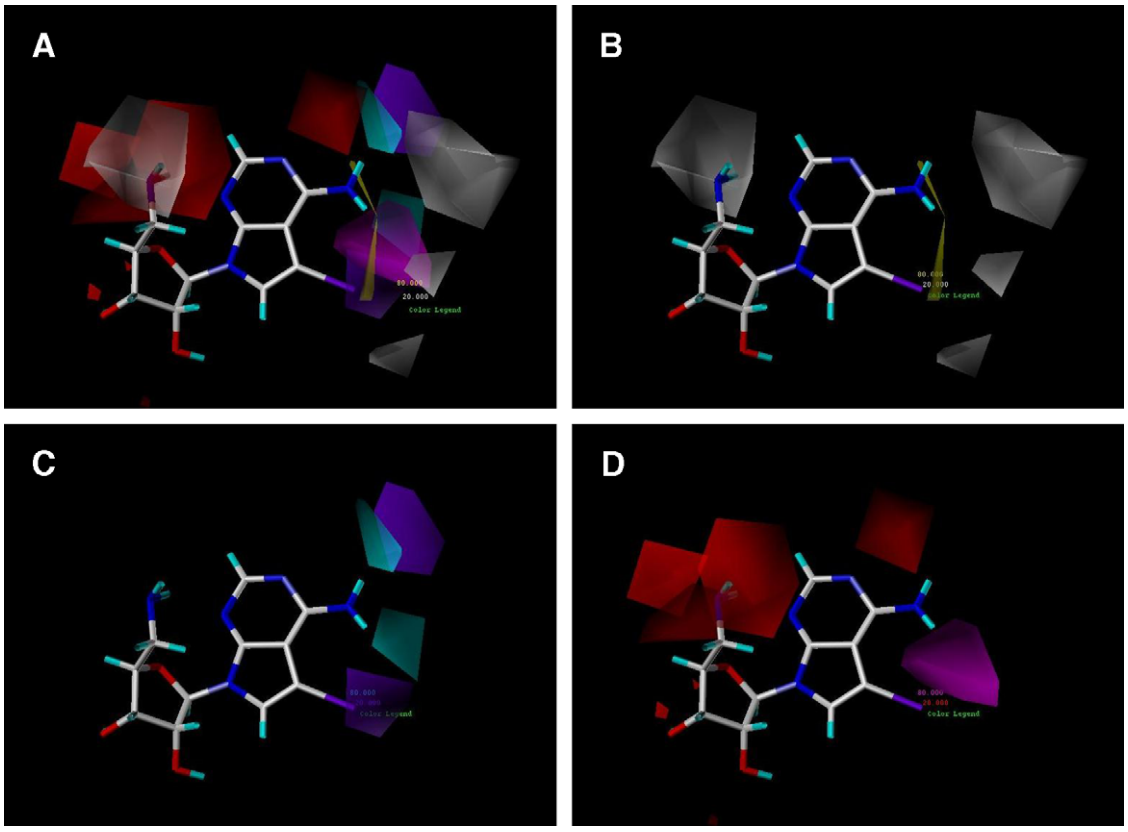

Figure 3. CoMSIA stdev * coeff contour maps for PPNs (CoMSIA-HDA model). Compound **26** is shown inside the field. (A) All the fields, (B) hydrophobic field, (C) H-bond donor field and (D) H-bond acceptor field. Yellow and white isopleths indicate regions where hydrophobic groups favored and disfavored the activity, respectively. Cyan and purple isopleths represent areas where H-bond donors are favored and disfavored, respectively. Magenta and red isopleths represent areas where H-bond acceptors are favored and disfavored, respectively.

tors favor the AK inhibitory activity. In that connection, PPNs which contain CH_3 group at this position have a poor AK inhibitory activity (compound **11**; $\log(10^3/IC_{50}) = 1.78$); by replacing the CH_3 by a H-bond acceptor carbonyl oxygen (compounds **13** and **32**) the activity increases ($\log(10^3/IC_{50})$ above 3). Finally, one red isopleth is located near C4-position of pyrrolo[2,3-*d*]pyrimidine and several ones are located near C5-position of β-D-ribofuranose (Fig. 3D), which represents areas where H-bond acceptors disfavor the AK inhibitory activity. According to these contours, groups containing H-bond acceptor atoms are disfavored at C4-position, and groups containing H-bond acceptor atoms such as CH_2OH and CH_2N_3 (compounds **1** and **14**; $\log(10^3/IC_{50})$ around 4.5) are less favorable than CH_3 group (compound **2**; $\log(10^3/IC_{50}) = 5.05$) at C5-position of β-D-ribofuranose for a highly AK inhibitory activity.

3. Conclusions

CoMSIA approach has been applied to derive quantitative relationships between the structure of PPN analogues and their AK inhibitory activity. The present study indicates that hydrophobic, H-bond donor, and H-bond acceptor CoMSIA fields are enough to describe fully the inhibitory activity of these compounds. When using these fields, a statistically meaningful model was derived. Thus, prediction of AK activities with sufficient accuracy should be possible. Moreover, an interpretation of the respective CoMSIA fields makes it possible to draw conclusions concerning the most appropriate substituents for C4 and C5 positions of pyrrolo[2,3-*d*]pyrimidine scaffold and C5-position of β-D-ribofuranose of the PPN analogues. This analysis can contribute to the knowledge of the relevant characteristics of these compounds as AK inhibitors for their potential application as anticonvulsant drugs.

4. Materials and methods

4.1. Datasets: source and prior preparation

The molecular structures and activities of 37 PPN analogues were taken from the literature.[12] The activities were collected and transformed into $\log(10^3/IC_{50})$ values. IC_{50} refers to the micromolar concentration of the compound required for 50% inhibition of the AK. The structures and biological activities used in this study are summarized in Table 1. Molecular modeling was performed using the Sybyl 7.2 software of Tripos.[24] All the molecules were sketched using the Biopolymer module in Sybyl. Each structure was fully geometry-optimized using a conjugate gradient procedure based on the TRIPOS force field[25] and Gasteiger–Marsili charges.[26] The settings of optimization are shown in Ta-

Table 3. Settings for the optimization of the molecules

Force field parameter set	Tripos
Charges	Gasteiger–Marsili
1–4 scaling	1
Dielectric function	Distance
NB cutoff	8
Dielectric constant	1
H-bond radius scaling	0.7
Method	Conjugate gradient
Max iterations	1000
Max displacement	0.01
Min energy change	0.05
Simplex threshold	1000
Termination	Gradient
Non-bonded reset	10
RMS displacement	0.001
Gradient	0.005

ble 3. Then, molecules were aligned by an atom-by-atom least-square fit. We used the pyrrolo[2,3-*d*]pyrimidine fragment of the active compound **27** in its optimized conformation as a template. The dataset was divided into two subdatasets. Five compounds were chosen randomly as a test set and were used for external validation of the 3D-QSAR models; the training sets included all the remaining 32 compounds.

4.2. CoMSIA models

For the CoMSIA calculations, molecules of the training set were placed in a rectangular grid and the interaction energies between a probe atom and all compounds were computed at the surrounding points, using a volume-dependent lattice with 2.0 Å grid spacing. Then, standard Sybyl parameters were used for a partial least squares (PLS) analysis. The number of components in the PLS models were optimized by using a Q^2 value, obtained from the leave-one-out (LOO) cross validation procedure, with the SAMPLS[27] sampling method. The number of components was increased until additional components did not increase Q^2 by at least 5% per added component. In the CoMSIA analyses, similarity is expressed in terms of steric occupancy, electrostatic interactions, local hydrophobicity, and H-bond donor and acceptor properties, using a 0.3 attenuation factor. The modeling capability (goodness of fit) was judged by the correlation coefficient squared, R^2. The prediction capability (goodness of prediction) was indicated by the cross-validated R^2 (Q^2). For a stronger evaluation of model applicability for prediction on new chemicals, the activities of the compounds of the test set were evaluated by using the best CoMSIA model.

Acknowledgments

This work was supported by 'Programa Bicentenario de Ciencia y Tecnología', ACT/24 (J.C. and F.D.G.N.).

References and notes

1. Jacobson, K. A.; van Galen, P. J. M.; Williams, M. *J. Med. Chem.* **1992**, *35*, 407.
2. Knutsen, L. J. S.; Murray, T. F. In *Purinergic Approaches in Experimental Therapeutics*; Jacobson, K. A., Jarvis, M. F., Eds.; Wiley-Liss: New York, 1997; pp 423–447.
3. Dunwiddie, T. V.; Worth, T. *J. Pharmacol. Exp. Ther.* **1982**, *220*, 70.
4. Phillis, J. W.; Wu, P. H. In *Physiology and Pharmacology of Adenosine Derivatives*; Daly, J. W., Phillis, J. W., Kuroda, Y., Shimizu, H., Ui, M., Eds.; Raven Press: New York, 1983; pp 219–236.
5. Malhotra, J.; Gupta, Y. K. *Br. J. Pharmacol.* **1997**, *120*, 282.
6. Foster, A. C.; Miller, L. P.; Wiesner, J. B. In *Purine and Pyrimidine Metabolism in Man, VII*; Sahota, A., Taylor, M., Eds.; Plenum Press: New York, 1995; pp 427–430.
7. Wiesner, J. B.; Ugarkar, B. G.; Castellino, A. J.; Barankiewicz, J.; Dumas, D. P.; Gruber, H. E.; Foster, A. C.; Erion, M. D. *J. Pharmacol. Exp. Ther.* **1999**, *289*, 1669.
8. Moser, G. H.; Schrader, J.; Deussen, A. *Am. J. Physiol.* **1989**, *256*, C799.
9. Pak, M. A.; Hass, H. L.; Decking, U. K. M.; Schrader, J. *Neuropharmacology* **1994**, *33*, 1049.
10. Gasteiger, J. *Anal. Bioanal. Chem.* **2006**, *384*, 57.
11. Pârvu, L. *J. Cell Mol. Med.* **2003**, *7*, 333.
12. Ugarkar, B. G.; DaRe, J. M.; Kopcho, J. J.; Browne, C. E., III; Schanzer, J. M.; Wiesner, J. B.; Erion, M. D. *J. Med. Chem.* **2000**, *43*, 2883.
13. Srikanth, K.; Debnath, B.; Jha, T. *Bioorg. Med. Chem. Lett.* **2002**, *12*, 899.
14. Hansch, C.; Fujita, T. *J. Am. Chem. Soc.* **1964**, *86*, 1616.
15. González, M. P.; Moldes, M. C. T. *Bioorg. Med. Chem. Lett.* **2004**, *14*, 3077.
16. Estrada, E.; Peña, A. *Bioorg. Med. Chem.* **2000**, *8*, 2755.
17. Todeschini, R.; Consonni, V. *Handbook of Molecular Descriptors*; Wiley-VCH: Weinheim, 2000.
18. Caballero, J.; Saavedra, M.; Fernández, M.; González-Nilo, F. D. *J. Agric. Food Chem.* **2007**, *55*, 8101.
19. Caballero, J.; Fernández, M.; Saavedra, M.; González-Nilo, F. D. *Bioorg. Med. Chem.* **2008**, *16*, 810.
20. Verma, R. P.; Hansch, C. *Bioorg. Med. Chem.* **2005**, *13*, 4597.
21. Devillers, J.; Lipnick, R. L. In *Practical Applications of Quantitative Structure–Activity Relationships (QSAR) in Environmental Chemistry and Toxicology*; Karcher, K., Devillers, J., Eds.; Kluwer: Dordrecht, 1990; pp 129–143.
22. Clark, R. D.; Sprous, D. G.; Leonard, J. M. In *Rational Approaches to Drug Design*. Höltje, H-.D., Sippl, W., Ed.; Prous Science SA, 2001, pp 475–485.
23. Mathews, I. I.; Erion, M. D.; Ealick, S. E. *Biochemistry* **1998**, *37*, 15607.
24. SYBYL, version 7.2; Tripos Inc.: 1699 South Hanley Road, St. Louis, MO 63144, USA.
25. Clark, M.; Cramer, R. D.; van Opdenbosch, N. *J. Comput. Chem.* **1989**, *10*, 982.
26. Gasteiger, J.; Marsili, M. *Tetrahedron* **1980**, *36*, 3219.
27. Bush, B. L.; Nachbar, R. B., Jr. *J. Comput. Aided Mol. Des.* **1993**, *7*, 587.